Measuring Frequency Characteristics of Linear Two-Port Networks Automatically

By JAMES G. EVANS

(Manuscript received November 2, 1968)

This paper presents a new automatic technique for complete linear characterization of transistors and general two-port devices from standard insertion and bridging measurements. This technique includes a calibration sequence and mathematical transformation to provide parameters independent of actual test set impedances, as well as a special hardware design which allows for convenient self-measurement of the test set impedances. Knowledge of these impedances is used to reduce the measured quantities to arbitrary device parameters referenced entirely to a set of calibration standards. This independence of the parameters from the measuring set impedances allows for considerable reduction in the design constraints on the test set impedances and device connecting jigs.

I. INTRODUCTION

In implementing a linear two-port device characterizing facility on the computer operated transmission measuring set, several factors had to be considered.[1] First, the advantages of automated measurements could be retained only if the switching required to obtain four independent measurement configurations were done automatically. Second, the implementation must be broadband to take advantage of the 50 Hz to 250 MHz frequency range of the measuring set. Finally, the measurement method must be inherently capable of utilizing the high accuracy of the measuring set. An implementation was chosen which uses standard insertion and bridging measurements.[2–4] This choice is particularly compatible with the above factors.

Insertion and bridging measurements are made with the unknown terminated in a nominal impedance environment, in the present instance 50 ohms. At this impedance level, broadband, solenoid-oper-

ated coaxial switches are available which introduce only minor reflections in 50 ohm transmission circuits. In the computer operated transmission measuring set such switches are extensively used to provide automatic commuting of the unknown among the four independent configurations in which measurements are made. By arranging relay switching so that dc bias can be continuously maintained when measuring active unknowns such as transistors, multiple warm-up periods are eliminated and thermal equilibrium must be reached only once. Another advantage of the 50 ohm environment surrounding the unknown is that transistors and other active devices tend to be stable when terminated resistively.

If the terminal impedances deviate from the 50 ohm nominal, measurement data which assumes 50 ohm impedances will be in error. In the past, these errors were minimized to the best degree practical by controlling the impedance environment around the unknown. Even so, the lack of ideal circuit elements meant that significant errors remain in linear characterization data. In the computer operated transmission measuring set, the circuit elements are even less ideal because of impedance deviations resulting from the large number of coaxial relays used. The impedance control problem is further aggravated by the difficulty of designing low reflection dc bias networks to operate over several decades of frequency. For the latter reason the frequency range of measurement for devices requiring dc bias is confined to between 50 kHz and 250 MHz. The total measurement errors that could conceivably result from the residual impedance deviations would prevent meeting our accuracy targets.

A solution to this problem, which represents an advance over past practice, was to endow the measurement facility with the capability to self-measure the source and load impedance deviations around the unknown, thereby permitting measurement data to be corrected for the residual mistermination.

The effect achieved in the execution of this technique is to refer the corrected data to a set of calibration standards. It is not necessary to have carefully controlled terminal impedances, and high accuracy characterizations are obtainable using device-connecting jigs with poor terminal impedances.

A further advantage of the new technique lies in the greater analytical ease of converting measured data to two-port characterization sets of most direct interest to the designer. In past measuring arrangements, measured insertion ratios $e^{\phi_{21}}$ and $e^{\phi_{12}}$ are related to relevant param-

eters by the equations[3,4]

$$e^{\phi_{21}} = \frac{1 - s_{22}\rho_L - s_{11}\rho_g - \rho_g\rho_L(s_{12}s_{21} - s_{11}s_{22})}{s_{21}(1 - \rho_g\rho_L)}$$

and

$$e^{\phi_{12}} = \frac{1 - s_{11}\rho_L - s_{22}\rho_g - \rho_g\rho_L(s_{12}s_{21} - s_{11}s_{22})}{s_{12}(1 - \rho_g\rho_L)},$$

where the generator and load and reflection coefficients, ρ_g and ρ_L, and the scattering parameters are referred to the nominal design impedance, generally 50 or 75 ohms in earlier cases. Similarly, expressions can be derived for the measured input and output reflection coefficients in terms of all four of the desired parameters and the terminating reflection coefficients. Even if the test set reflection coefficients could be determined by independent measurement, the desired parameters cannot be obtained without recourse to a difficult mathematical inversion or a lengthy iterative calculation upon four coupled equations.

One of the important attributes of the new approach discussed in this paper is that the desired S parameters are explicitly dependent on known quantities and hence easily evaluated. This is made possible by initially finding the scattering parameters of the unknown, referred to the actual test set source and load impedances, as described in Section II.

II. MEASUREMENT AND IMPLEMENTATION

2.1 S *Parameter Representation*

The insertion and bridging measurement data are closely related to scattering parameters. (See Appendix A.) It should be recalled that there are several types of scattering parameters.[5-7] The calculations which follow deal exclusively with voltage scattering parameters. In the present context, these parameters are defined with respect to the terminal impedances which actually prevail in the test set. The voltage S parameters along with their normalizing impedances can be transformed to any other parameter representation by well known transformations.[5]

2.2 *Measurement of* s_{12} *and* s_{21}

The transmission S parameters, s_{12} and s_{21}, are obtained almost directly from the insertion measurement illustrated in Fig. 1. With

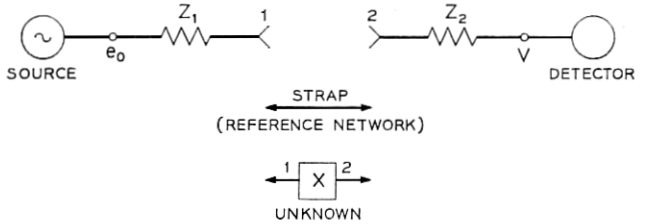

Fig. 1 — Model of S_{12}, S_{21} measurement. Circuit shown for S_{21} measurement; detector and source interchanged for S_{12} measurement.

the unknown inserted in the measuring network the detected voltage V is directly proportional to s_{21} of the unknown defined with respect to the normalizing impedances Z_1 and Z_2. (See Appendix A.)

$$\{s_{21}\}_{z_1,z_2} = \{R_{21} \cdot V\}_X \,. \tag{1}$$

The constant of proportionality R_{21} can be determined by inserting a reference network with known s_{R21}

$$\{s_{21}\}_{z_1,z_2} = \{s_{R21}\}_{z_1,z_2} \frac{V_X}{V_R}. \tag{2}$$

Typically the reference network is a coaxial line of known electrical length. When ports 1 and 2 can be directly connected the line is of zero length for which s_{R21} takes the simple form

$$\{s_{R21}\}_{z_1,z_2} = \frac{2 \cdot Z_2}{Z_1 + Z_2}. \tag{3}$$

This result can be seen directly or derived from equation (31) in Appendix C. The results for a reference line of finite length are derived as an example in Appendix C.

The hardware implementation is such that the impedances seen to the left and right of the unknown are essentially the same for s_{12} and s_{21} measurement. This invariance of the terminal impedances, with respect to interchange of the source and detector, is accomplished by using a pair of judiciously located 20 dB pads. The hardware details are described in Section 2.5. The measurement of s_{12} is similar to that of s_{21}. For this case,

$$\{s_{12}\}_{z_1,z_2} = \{s_{R12}\}_{z_1,z_2} \frac{V_X}{V_R}. \tag{4}$$

2.3 *Measurement of* s_{11} *and* s_{22}

The quantity s_{11} of an unknown device is obtained indirectly by a bridging measurement. For this measurement the source and detector are directly connected as illustrated in Fig. 2. The device to be measured, as well as the calibration standards, are successively bridged across the source-detector interconnection. The implementation is such that the impedance seen at terminal 2 is Z_2, the same impedance as for the previously described s_{12} and s_{21} measurement.

The quantity s_{11} is determined by making four measurements of V. Three consist of calibration measurements using open, short, and reference impedance standards. The fourth measurement is made with the unknown connected. These measurements can be combined to obtain a reflection coefficient

$$\{s_{11}\}_{Z_R, Z_2}$$

closely related to the desired

$$\{s_{11}\}_{Z_1, Z_2}.$$

$$\{s_{11}\}_{Z_R, Z_2} = \frac{(V_X - V_R)(V_\infty - V_0)}{(V_\infty - V_R)(V_X - V_0) + (V_R - V_0)(V_\infty - V_X)}. \tag{5}$$

The term

$$\{s_{11}\}_{Z_R, Z_2}$$

does not have the desired impedance normalization on port 1. The desired result is obtained through the transformation

$$\{s_{11}\}_{Z_1, Z_2} = \left\{\frac{s_{11} - \Gamma_1}{1 - \Gamma_1 \cdot s_{11}}\right\}_{Z_R, Z_2} \tag{6}$$

where

$$\Gamma_1 = \frac{Z_1 - Z_R}{Z_1 + Z_R} \tag{7}$$

is obtained from an additional measurement described in Section 2.4. Notice that Γ_1 is the reflection coefficient of Z_1 normalized with respect to Z_R. Hence, once Z_1 becomes known, all of the information is available to compute the value of $\{s_{11}\}_{Z_1, Z_2}$. The quantity s_{22} is determined in an analogous manner. In this case the hardware implementation is such that the impedance terminating port 1 of the unknown is Z_1, the same impedance as in the s_{12} and s_{21} measurements; it is seen that the

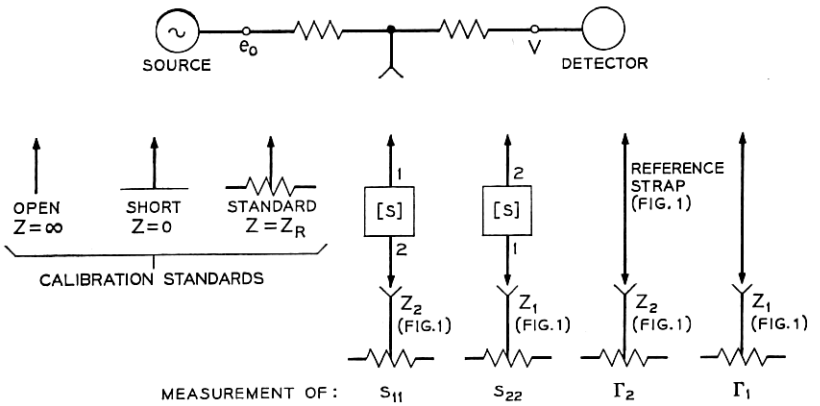

Fig. 2 — Model of S_{11}, S_{22}, Γ_1, and Γ_2 measurement.

measured data this time yield s_{22} with respect to Z_1 at port 1 and Z_R at port 2. The term $\{s_{22}\}_{Z_1,Z_2}$ is then determined as before, as a function of the four measured detector voltages and Γ_2, where

$$\Gamma_2 = \frac{Z_2 - Z_R}{Z_2 + Z_R}. \tag{8}$$

(Appendix B shows that the equations of Section 2.3 are general and apply for any linear network interconnecting the source, the detector, and the unknown.)

The above discussion has described a procedure for determining the four voltage scattering parameters $\{s\}_{Z_1,Z_2}$. This set can be transformed to a more useful parameter representation only if Z_1 and Z_2 or equivalently Γ_1 and Γ_2 can be determined. Section 2.4 discusses the procedure for determining Γ_1 and Γ_2.

2.4 *Measurement of* Γ_1 *and* Γ_2

The measurement procedure for determining Γ_2 is similar to that for evaluating s_{11}. With the reference transmission strap used in the s_{12} and s_{21} measurements inserted in the bridging configuration of Fig. 2 and terminated in Z_2, the detected voltage is V_{Γ_2}. The reflection coefficient computed from equation (5) with V_X replaced by V_{Γ_2} is the reflection coefficient of Z_2, with respect to Z_R, as viewed through the reference strap, which has known transforming properties. When ports 1 and 2 can be directly connected the line section is of zero length for which the transformation is unity. In this event the reflection coefficient com-

puted from equation (5) is equal to Γ_2 . The term Γ_1 is evaluated in a similar manner using the s_{22} bridging configuration.

Notice that Z_1 and Z_2 can be determined on a broadband basis simply with two additional calibration measurements. It is important to realize that this is possible only because of the particular physical embodiment which results in the network being terminated in Z_2 on port 2 during the s_{12}, s_{21}, and s_{11} measurements and in Z_1 on port 1 during the s_{12}, s_{21}, and s_{22} measurements. Section 2.5 describes the hardware arrangement. Notice that for an arrangment in which the terminal impedances remain invariant under all four S measurement conditions these two additional measurements are redundant. In this case, the terminal impedances can be determined from the open, short, and standard impedance measurements. (See Ref. 8.)

2.5 *Physical Embodiment*

Figure 3 is a simplified schematic diagram of the 2-port linear characterization facility. The components L_1, C_1, L_2, and C_2 comprise the bias networks necessary for supplying dc bias to devices such as transistors. The attenuators P_1 and P_2 have an insertion loss of 20 dB. These attenuators play a critical role in maintaining the terminal impedance constancy described earlier.

The coaxial switch closures and the circuit paths of a s_{21} measurement are specifically shown in Fig. 4. The terminal impedances seen to the left and right of ports 1 and 2 are Z_1 and Z_2, respectively. A simple examination of Fig. 3 will reveal that the switch closures and paths inside P_1 and P_2 are identical for the s_{12} and s_{21} measurements. The switching necessary to convert to the s_{12} measurement changes the reflection coefficient seen looking to the left of P_1 and right of P_2 by less than 0.1. These changes are attenuated by P_1 and P_2 so that the changes in Γ_1 and Γ_2 seen at the terminals 1 and 2, respectively, are less than 0.001. Within the bounds of neglecting a possible 0.001 change, Γ_1 and Γ_2, and therefore Z_1 and Z_2, are invariant under the change from the s_{21} to the s_{12} measurement.

Figure 5 illustrates the switch closures and circuit paths of an s_{22} measurement. Attenuator P_2 has been eliminated from this measurement to prevent a loss in measurement resolution. Notice that all switch closures and circuit paths between terminal 1 and attenuator P_1 are the same as in the s_{12} and s_{21} measurements. The reflection coefficient seen to the left of P_1 has changed less than 0.1 in switching into this measurement mode. Therefore, the reflection

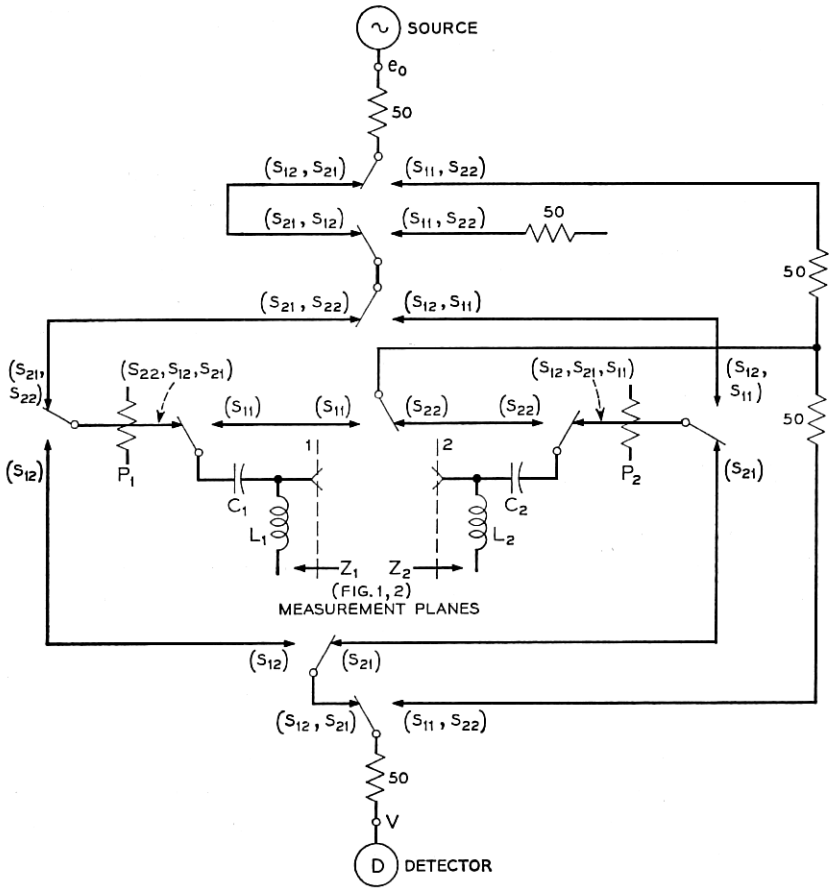

Fig. 3 — Simplified schematic of transistors measurement unit. Signal routing required to set up measurement paths for the determination of S_{12}, S_{21}, S_{11}, or S_{22} are shown for each switch.

coefficient seen looking into terminal 1 cannot differ from Γ_1 by more than 0.001, a negligible amount. A similar analysis of the s_{11} measurement mode reveals that the reflection coefficient seen looking into terminal 2 cannot differ from Γ_2 by more than 0.001.

2.6 *Other Parameter Representations*

The set $\{s\}_{Z_1, Z_2}$, $Z_1(\Gamma_1)$ and $Z_2(\Gamma_2)$ is a well defined voltage scattering parameter representation of the linear characteristics of the 2-port unknown. This representation has no practical application, but it can

be easily converted to a more useful representation by well known transformations (Ref. 6). One particularly useful and easily obtained parameter set is the voltage scattering parameters normalized to 50 ohms ($Z_R = 50$ ohms). This set is obtained from the measured set by use of the transformations of Appendix C:

$$\{s_{11}\}_{Z_R, Z_R} = \left\{ \frac{\Gamma_1 + s_{11} + \Gamma_1\Gamma_2 s_{22} + \Gamma_2\,\Delta s}{1 + \Gamma_1 s_{11} + \Gamma_2 s_{22} + \Gamma_1\Gamma_2\,\Delta s} \right\}_{Z_1, Z_2} \tag{9}$$

$$\{s_{12}\}_{Z_R, Z_R} = \left\{ \frac{s_{12}(1 - \Gamma_1)(1 + \Gamma_2)}{1 + \Gamma_1 s_{11} + \Gamma_2 s_{22} + \Gamma_1\Gamma_2\,\Delta s} \right\}_{Z_1, Z_2} \tag{10}$$

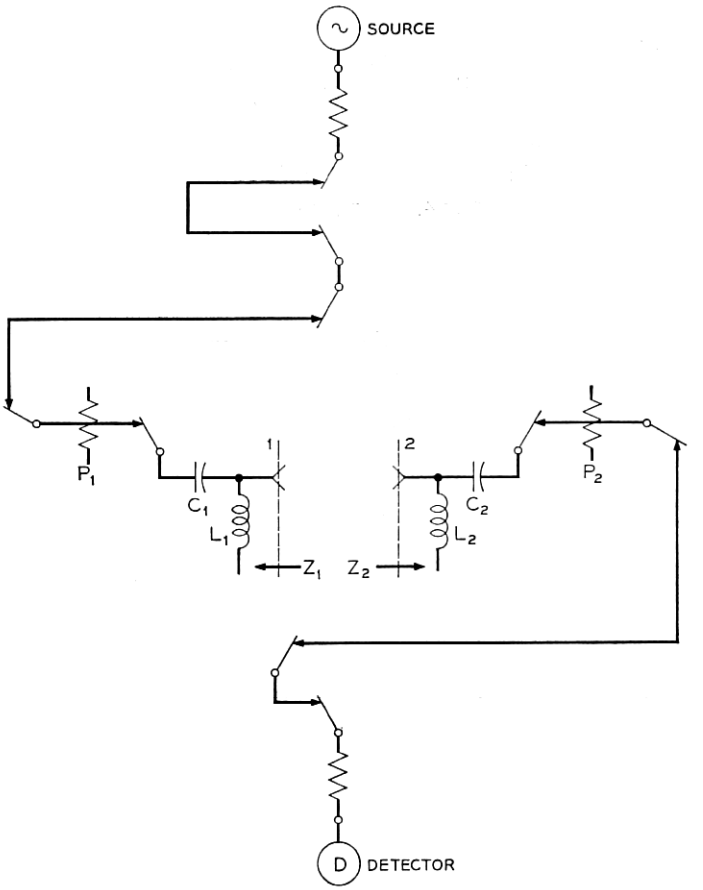

Fig. 4 — Path through transistor measurement unit for S_{21} evaluation.

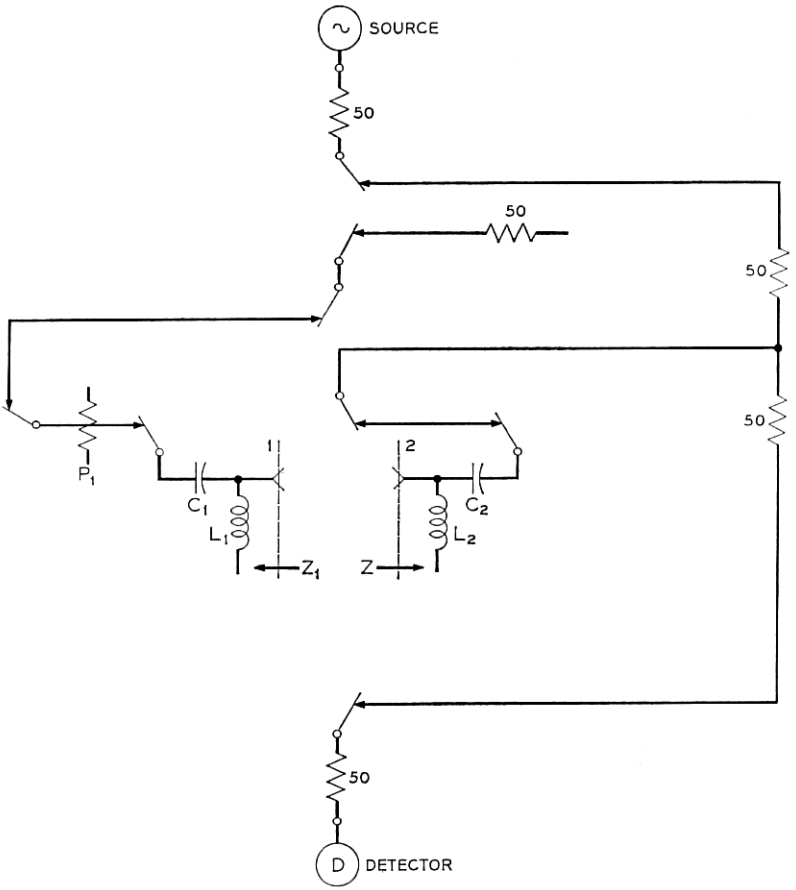

Fig. 5 — Path through transistor measurement unit for S_{22} evaluation.

$$\{\Delta s\}_{Z_1,Z_2} = \{s_{11}s_{22} - s_{12}s_{21}\}_{Z_1,Z_2} . \tag{11}$$

The transformations for s_{22} and s_{21} are found by transposing subscripts in the above equations. It is useful to realize that since the transformed S parameters are normalized to equal real impedances they are numerically equal to the current and power scattering parameters with the same normalization.

The transformed parameters are independent of Z_1 and Z_2, depending only upon the open, short, Z_R, reference network calibration standards and the loss and phase measurement accuracy of the test set. This

independence from Z_1 and Z_2 allows for useful freedom in the design of the measuring apparatus terminal impedances.

III. SPECIAL CALIBRATION FEATURES

In Section II a measurement technique has been presented in which the linear characteristics of a 2-port unknown are determined relative to four calibration standards. An idealized set consisting of an open, short, standard impedance and a zero length line were treated for mathematical simplicity. The calibration standards used with the automated facility deviate considerably from this idealized set over the broad frequency range of interest. A failure to compensate for these deviations would adversely affect the accuracy of linear characterization. Compensation is accomplished by modeling the deviations as a function of frequency and then computationally accounting for them in the data reduction program.

3.1 *Compensation for a Transmission Reference Line of Nonzero Length*

Physical constraints often make it impossible to directly interconnect ports 1 and 2 for the measurements needed for the determination of s_{12}, s_{21}, Γ_1 and Γ_2. Interconnection is achieved in these cases by using a short transmission line with a characteristic impedance equal to Z_R and an electrical length equal to θ. For this network

$$\{s_{R12}\}_{Z_R, Z_R} = \{s_{R21}\}_{Z_R, Z_R} = e^{-i\theta},$$

where θ is computed from the line constants and length.

For determining Γ_1 and Γ_2 this line has a particularly simple transforming property. Γ_1 and Γ_2 when viewed through the line appear as $\Gamma_1 e^{-i2\theta}$ and $\Gamma_2 e^{-i2\theta}$, respectively.

In the actual measurements, determining s_{12} and s_{21} of the unknown require s_{R12} and s_{R21} of the line normalized with respect to Z_1 and Z_2. These quantities are obtained by transforming from the (Z_R, Z_R) impedance normalization to the (Z_1, Z_2) impedance normalization as illustrated in Appendix C. The data reduction program allows for reference lines of arbitrary length.

3.2 *Compensation for Nonideal Bridging Calibration Standards*

Typically high quality standard impedance (Z_R) terminations are available whose deviations from nominal are negligible. This is not true for the open and short calibration standards. Mechanical consider-

ations sometimes require that the short and open reference planes be displaced from the measurement plane by a section of transmission line. In addition, the "open" differs from ideal by a fringing capacitance. For small reactive perturbations or arbitrary displacements in a transmission line of characteristic impedance Z_R, the actual open and short circuit reflection coefficients are of the simple form

$$\Gamma_\infty \mid_{Z_R} = e^{-2j\tau_\infty \omega} \tag{12}$$

$$\Gamma_0 \mid_{Z_R} = -e^{-2j\tau_0 \omega} \tag{13}$$

where τ_∞ and τ_0 are the time delays for the lengths of line involved, including a correction for fringing capacitance at the end. The linear dependence of the reflection phase angles on frequency facilitates broadband computational correction. In the data reduction program a more general bridging equation than equation (5) (see Appendix B) is programmed to allow for calibration standards of the above form.

3.3 *Measurement Plane Translations*

For some unknowns it is desirable to define the reference planes of the S parameters translated down 50 ohm transmission lines from the measurement planes. Examples are the air line measurements in Section 5.1, and the case of measuring an integrated circuit connected to the test set by 50 ohm microstrip transmission lines of significant electrical length when information about the chip alone is sought. (An alternative approach to characterization would be to develop integrated circuit standards so that calibration could be performed at the chip interface.) Analysis shows that the presence of transmission lines of electrical length α are accounted for within the previously developed mathematical framework by entering the translated angles $-\omega\tau_\infty + 2\alpha$, $-\omega\tau_0 + 2\alpha$ and $\theta - 2\alpha$ instead of the physical angles $-\omega\tau_\infty$, $-\omega\tau_0$ and θ into the data reduction program. The alternative approach, requiring additional programming, would "remove" the transmission lines by appropriate matrix manipulations.

IV. STATEMENT OF ERRORS IN $S_{50,50}$ PARAMETERS

This section gives the results of an approximate worst case error analysis for $S_{50,50}$ parameters. The analysis was performed on these parameters because of the mathematical simplifications resulting from their similarity to the measured quantities. The results are derived by assuming that Γ_1, Γ_2, and the fundamental error terms are small compared with unity. This approximation allows for simplification of the equations presented in the earlier sections. The fundamental error terms

are added on a worst case basis to obtain overall error bounds. The lengthy analysis has been omitted for brevity.

4.1 *Bound for the* s_{11} *and* s_{22} *Measurements*

The errors in the s_{11} and s_{22} measurement arise from two principal sources, those associated with the bridging technique and those from interaction with the termination of the unknown. For an unknown with $| s_{12} \cdot s_{21} | \ll 1$ the latter error source is negligible and the bound for errors in the determination of s_{11} is,

$$| \Delta s_{11} |_{50,50} < \{0.0023 + 0.0023 | 1 - s_{11}^2 | + 0.0013 | s_{11} | | 1 + s_{11} | + 0.0013 | s_{11} | | 1 - s_{11} | + | \Gamma_s | | 1 - s_{11}^2 | \}_{50,50} \quad (14)$$

Implicit in equation (14) is the assumption that the uncertainties in the phase angles of the open and short circuit standards are less than 0.02 degree.

$$\Gamma_s = \frac{Z_R - 50}{Z_R + 50}. \quad (15)$$

Γ_s is the reflection coefficient of Z_R with respect to 50 ohms, which independent measurements have shown to be less than 0.005. Notice that certain terms in equation (14) disappear when s_{11} equals 0, -1, and 1. This reduction of the error bound occurs when the bridging measurement of the unknown reduces to a differential comparison of the unknown with either the 50 ohm, short, or open standard.

When the product $s_{12} \cdot s_{21}$ is not negligible, errors that occur in determining the reflection coefficient of the termination, Γ_2 for the s_{11} measurement, are transformed through the unknown to increase the error of the s_{11} determination. If $\Delta\Gamma_2$ is the error in determining Γ_2, the term

$$| \Delta\Gamma_2 | | s_{12} \cdot s_{21} |_{50,50} \quad (16)$$

must be added to equation (14) to account for this second error source. Since Γ_2 is determined from a bridging measurement, the bound on $\Delta\Gamma_2$ can be computed directly from equation (14) for $\Gamma_2 \ll 1$.

$$| \Delta\Gamma_2 | < 0.005 + | \Gamma_s | < 0.01. \quad (17)$$

If Γ_2 were not determined by measurement, then $\Delta\Gamma_2$ in equation (16) would have to be replaced by the worst case estimate of the value of Γ_2. From Fig. 6, Γ_2 is seen to be as large as 0.08. The error term of equation (16) is eight times larger in this case.

The relationship for Δs_{22} is found by changing subscripts.

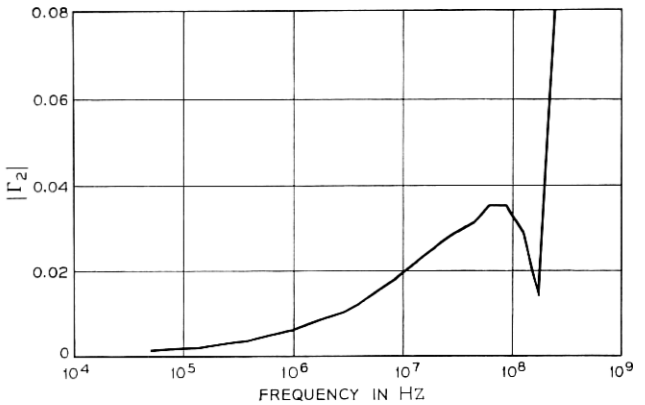

Fig. 6 — Test set port 2 reflection coefficient defined with respect to 50 ohms.

4.2 *Error Bound for the* S_{12} *and* S_{21} *Measurement*

The worst case fractional error in the determination of s_{12} is

$$\left|\frac{\Delta s_{12}}{s_{12}}\right|_{50,50} < \{0.0013 + 0.0013/|s_{12}| + |\Delta\theta| + |\Delta\Gamma_1| \cdot |s_{11}| + |\Delta\Gamma_2| \cdot |s_{22}|\}_{50,50} \quad (18)$$

The term that increases as $|s_{12}|$ decreases shows the intuitively appealing result that the relative error bound increases as the signal-to-noise ratio decreases. The term $\Delta\theta$ is the uncertainty in the electrical length of the reference network (zero line). The value of $\Delta\theta$ is less than 0.001 radians for the typical reference transmission line network. When direct interconnection of the measurement ports is possible, θ and therefore $\Delta\theta$, equals zero.

The terms $\Delta\Gamma_1$ and $\Delta\Gamma_2$ arise from the uncertainties in the knowledge of the terminating reflection coefficients, Γ_1 and Γ_2. The terms $\Delta\Gamma_1$ and $\Delta\Gamma_2$ are less than 0.01, as described in Section 4.1.

If Γ_1 and Γ_2 are not determined by measurement then $\Delta\Gamma_1$ and $\Delta\Gamma_2$ in equation (18) must be replaced by worst case values for Γ_1 and Γ_2. From Figs. 6 and 7, Γ_1 and Γ_2 are as large as 0.08 resulting in an eight fold increase in the mistermination terms of equation (18).

V. MEASUREMENTS TO CONFIRM ACCURACY

The two-port properties of a precision air-line, a precision attenuator, and a common base transistor were measured. These unknowns

are useful for demonstrating the accuracy of small signal characterization over a wide range of test parameter magnitudes.

5.1 *Characterization of a Precision* 30-cm *Air Line*

A General Radio 900-L30 precision 14 mm air line was measured on the automated facility and the data processed to yield scattering parameter data. The calibration standards consisted of a General Radio 90-W50 coaxial 50 ohm standard, a General Radio 900-WN coaxial short circuit, a coaxial open circuit, and a zero length line. The test set measurement ports (General Radio 900) were at the ends of flexible cable, thus allowing direct interconnection for the reference insertion ("zero-line") measurement. The open circuit standard, consisting of an unterminated General Radio 900 connector, was corrected for 0.16 pF of fringing capacitance by the techniques of Section 3.2.

The $s_{50,50}$ ohm parameters of the line were computed. This matrix is symmetrical and therefore only s_{11} and s_{12} data are presented in Figs. 8 through 11. The results for an ideal air line are $s_{11} = 0$ and $s_{12} = e^{-j\omega\tau}$, where $\omega\tau$ equals 90° at 250 MHz. To expose the errors of measurement, the reference plane translation technique of Section 3.3 was used to remove the linear phase component from all the S parameters. Alternatively, the translation is equivalent to multiplying each matrix element by $e^{j\omega\tau}$. For an ideal air line the resulting $s_{50,50}$ parameters are $s_{11} = 0$ and $s_{12} = 1$. The data in Figs. 8 through 11 indicate how the actual air line deviates from these ideal values.

The deviations can be accounted for by skin effect losses. The high

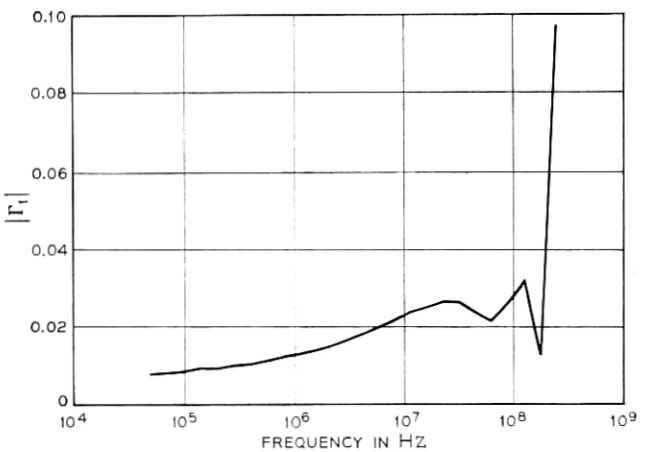

Fig. 7 — Test set port 1 reflection coefficient defined with respect to 50 ohms.

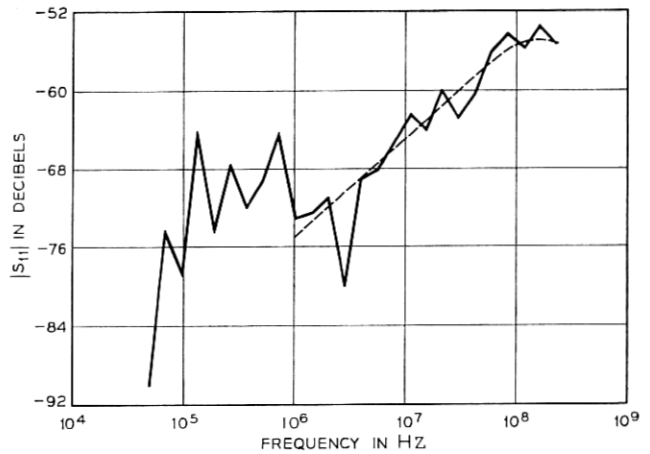

Fig. 8 — Magnitude of $S11_{50,50}$ for a precision 30 cm airline with the linear phase component subtracted.

frequency (1 MHz or greater for this example) $s_{50,50}$ parameters for a transmission line deviating from the ideal because of skin losses are derived in Appendix D. Multiplication of these parameters by $e^{j\omega\tau}$ converts them to a form compatible with the figures.

$$\{s_{11}\}_{50,50} = \lambda(z\omega\tau)^{\frac{1}{2}}\left(\frac{\sin \omega\tau}{\omega\tau}\right) \exp\,(j^{\pi/4}) \tag{19}$$

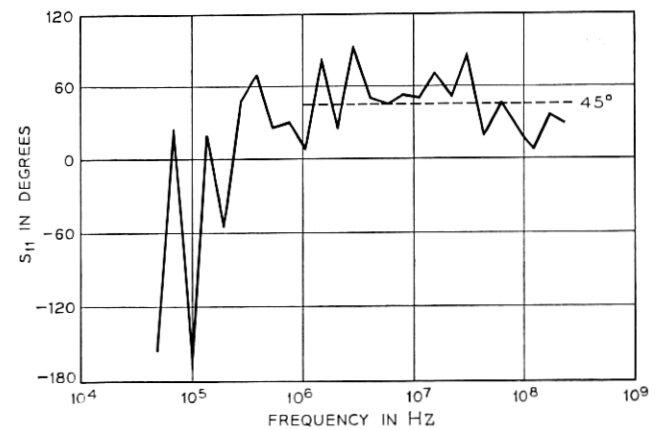

Fig. 9 — Phase of $S11_{50,50}$ for a precision 30 cm airline with the linear phase component subtracted.

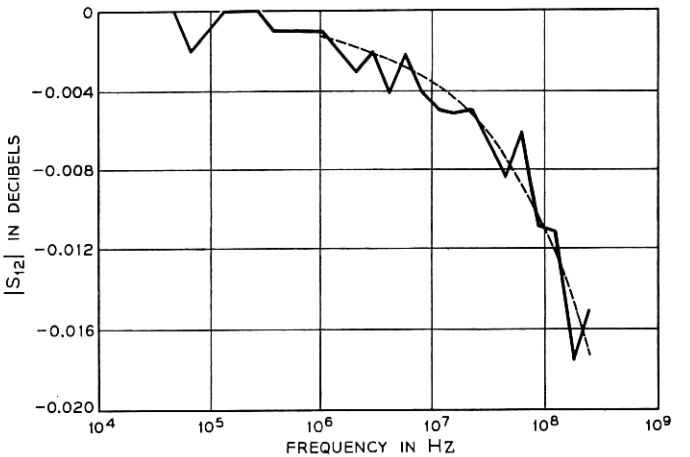

Fig. 10 — Magnitude of $S12_{50,50}$ for a precision 30 cm airline with the linear phase component subtracted.

$$\{s_{12}\}_{50,50} = \exp\left[-\lambda(\omega\tau)^{\frac{1}{2}}\right] \exp\left[-j\lambda(\omega\tau)^{\frac{1}{2}}\right] \tag{20}$$

where λ is a frequency independent, skin effect parameter dependent on surface conductivity as well as other line parameters. The value of λ was determined to be 0.0016 by fitting the magnitude of s_{12} from equation (20) to the measured results. The smooth curve in Fig. 10 shows that the fit to the magnitude of s_{12} is typically better than 0.002 dB. Using this value of λ, the phase of s_{12} and the magnitude of s_{11} were computed. The results are plotted in the Figs. 8 and 11.

The deviations of the measured results from the theoretical skin loss curves are estimators of characterization accuracy. Most of the deviations result from the sensitivity limits of 0.001 dB and 0.01°. The observed deviations are an order of magnitude smaller than the worst case errors predicted by the equations of Sections 4.2 and 4.3. If the mistermination corrections were not performed, the errors in s_{11} and s_{22} would be substantially larger. For example s_{11} would be virtually equal to Γ_2, the reflection coefficient of port 2. The values of Γ_2 are plotted in Fig. 7, showing that the resulting error in s_{11} could be as large as 0.08.

5.2 *Characterization of a Precision Attenuator*

A General Radio 900-G6 precision 14 mm 6 dB attenuator was measured and the data processed to obtain $s_{50,50}$ parameters. The true value

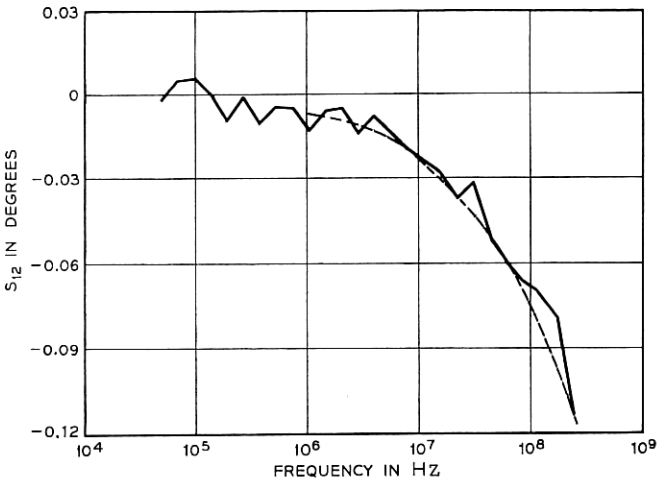

Fig. 11 — Phase of $S12_{50,50}$ for a precision 30 cm airline with the linear phase component subtracted.

of these parameters are not sufficiently well known for the attenuator to be used as a measurement standard. However, its measurement is useful in verifying characterization accuracy by comparing s_{12} and s_{21}. The terms $\{s_{12}\}_{50,50}$ and $\{s_{21}\}_{50,50}$ must be equal for a reciprocal network; $\{s_{12}\}_{Z_1, Z_2}$ and $\{s_{21}\}_{Z_1, Z_2}$ are in general not equal since typically $Z_1 \neq Z_2$. Therefore, the agreement between the 50 ohm S parameters is a measure of the success to which $\{s_{12}\}_{Z_1,Z_2}$, $\{s_{21}\}_{Z_1,Z_2}$, Z_1, and Z_2 have been determined.

The magnitudes of s_{12} and s_{21} are plotted in Fig. 12 for comparison. The midfrequency values for s_{12} and s_{21} are close to the dc measured value of -6.0151 dB. The attenuation bump below 10^4 Hz is from a poorer test set audio frequency signal-to-interference ratio. The agreement between s_{12} and s_{21} over most of the 400 Hz to 250 MHz range is better than a few thousands of a dB. In Fig. 13 the difference between the phase angles of these two parameters is plotted. The typical agreement is again excellent, better than several hundredths of a degree. The above differences are well within the 0.035 dB and 0.23° fractional error bounds on s_{12} and s_{21} computed from equation (18)

5.3 *Common Base Transistor Measurement*

A medium-power silicon transistor was measured in the common base configuration. The measurement data were then processed to

obtain common emitter h parameters by way of illustrating the flexibility of the data reduction program. The parameter h_{21} (or β) with and without mistermination errors is shown in Figs. 14 and 15. Differences between the corrected and uncorrected data as large as 5 dB and 20° are readily apparent. Discrepancies of this magnitude result from the β^2 multiplication of errors which occurs when converting common base parameters to common emitter parameters. Notice that the discrepancies decrease as the magnitude of β decreases. The agreement between corrected common emitter β curves derived from measurements in the common base, common collector, or common emitter modes is typically better than 1 dB and 5°. (See Ref. 1, Fig. 25.)

VI. SUMMARY

Complete device characterization can be rapidly and accurately achieved by the measurement method described in this paper. Loss of accuracy caused by nonideal test set terminations is virtually eliminated by measuring the deviations from ideal. The errors that arise are now the result of the smaller inaccuracy in measuring the deviations rather than to the gross deviations themselves. The self-measurement of the termination deviations is done at any frequency by two extra calibration measurements.

All measurements refer to a set of calibration standards, thereby making the derived parameters independent of the impedance properties of the test set. This attribute should facilitate the measurement

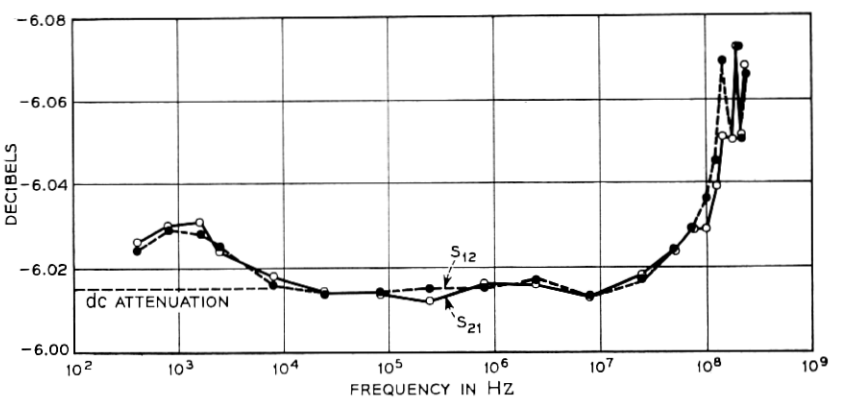

Fig. 12 — $|S_{12}|$ and $|S_{21}|$ of a precision 6 dB coaxial attenuator.

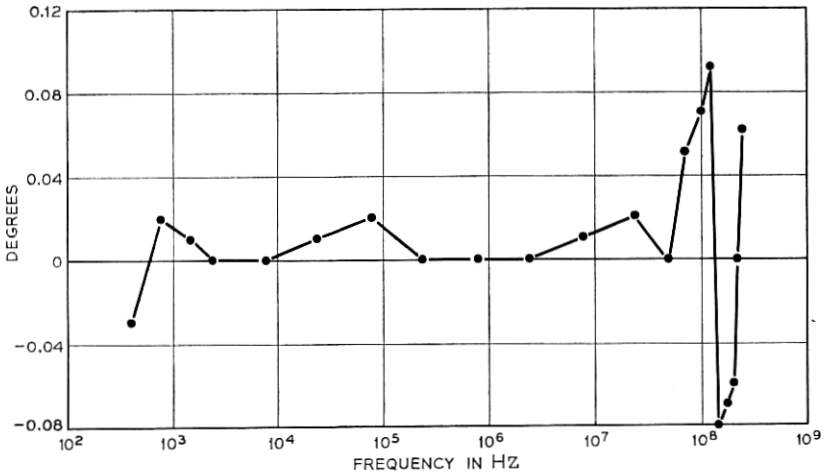

Fig. 13 — Angle of S_{21} minus the angle of S_{12} for the precision 6 dB coaxial attenuator.

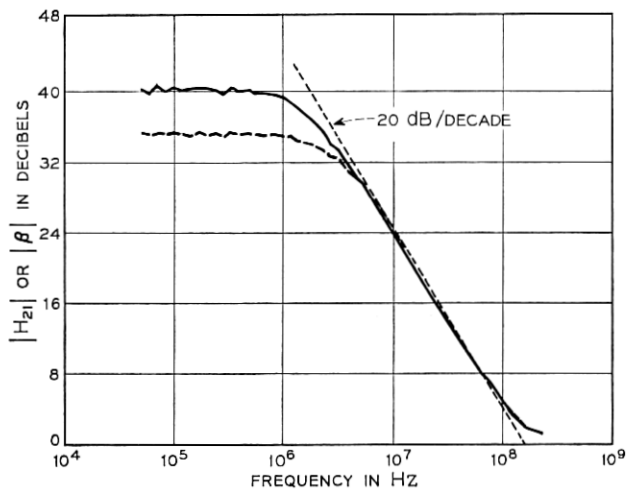

Fig. 14 — Common emitter $h21$ parameter computed from a common base measurement configuration. Mistermination errors are removed from the dashed curve and not from the solid curve.

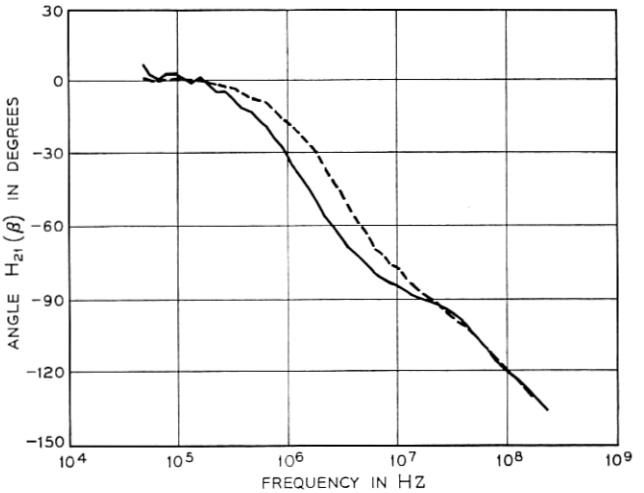

Fig. 15 — Common emitter $h21$ parameter computed from a common base measurement configuration. Mistermination errors are removed from the dashed curve and not from the solid curve.

of integrated circuits, for only the integrated calibration standards and not the connecting jig determine the accuracy of measurement.

VII. ACKNOWLEDGMENTS

R. G. Conway is responsible for a considerable portion of the mechanical design and assembly. The bridging equation deviation is an extension of the work of G. F. Critchlow. The author is especially indebted to G. D. Haynie and D. Leed for helpful criticism and advice.

APPENDIX A

Voltage Scattering Parameters

A network can be characterized in terms of traveling waves at selected reference planes rather than in terms of currents and voltages. Voltage scattering parameters are one such traveling wave representation. These parameters relate the reflected voltages from a network to the incident voltages. The matrix notation for this relationship for a two-port network is

$$\begin{bmatrix} V_{1r} \\ V_{2r} \end{bmatrix} = \begin{bmatrix} s_{11} & s_{12} \\ s_{21} & s_{22} \end{bmatrix} \Bigg|_{Z_1, Z_2} \begin{bmatrix} V_{1i} \\ V_{2i} \end{bmatrix}. \tag{21}$$

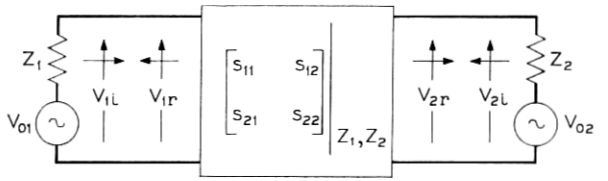

Fig. 16 — Scattering coefficient representation of a two-port network.

V_{1i} and V_{2i} are the incident voltage waves appearing at the port 1 and port 2 reference planes, respectively. V_{1r} and V_{2r} are the respective reflected voltage waves. The S parameters relating to the incident and reflected waves are defined with respect to the incident waves source impedances, Z_1 and Z_2.

The incident waves are related to the source potentials V_{01} and V_{02} (see Fig. 16) as follows,

$$V_{1i} = V_{01}/2 \qquad V_{2i} = V_{02}/2. \tag{22}$$

The conventional voltages appearing at ports 1 and 2 are

$$V_1 = V_{1i} + V_{1r} \qquad V_2 = V_{2i} + V_{2r}\,. \tag{23}$$

From equations (21), (22), and (23) it is easy to verify that

$$V_2 = \{(V_{01}/2)s_{21}\}_{Z_1,Z_2} \tag{24}$$

when $V_{02} = 0$. Therefore V_2 is directly proportional to $\{s_{21}\}_{Z_1,Z_2}$ when the network is inserted between a source of impedance Z_1 and a load of impedance Z_2 . Also when $V_{02} = 0$ the reflection coefficient defined as V_{1r}/V_{1i} is equal to $\{s_{11}\}_{Z_1,Z_2}$.

APPENDIX B

The Bridging Technique

The bridging technique is one method of determining the input and output scattering parameters of a device. This technique requires an oscillator, a detector, three impedance standards and an arbitrary three-port linear network. The judicious selection of this network will lead to better measurement sensitivity.

The essentials of a bridging measurement are illustrated in Fig. 17. Z and E_{03} comprise the Thévenin's equivalent circuit of port 3, the measurement port. An analysis shows that the detected voltage V remains unchanged if the unknown impedance Z_X is replaced by the

load and controlled source combination shown.

$$\Gamma = \frac{Z_X - Z}{Z_X + Z}. \tag{25}$$

Since the interconnecting network is linear,

$$V = A \cdot E + B \cdot \Gamma \cdot E_{03} \tag{26}$$

and

$$E_{03} = C \cdot E. \tag{27}$$

A, B, and C are system constants. Equation (26) is therefore seen to reduce to the form

$$V = a + b \cdot \Gamma \tag{28}$$

where $a = A \cdot E$ and $b = B \cdot C \cdot E$.
This equation has three unknowns, the two constants a and b, and the normalizing impedance Z. These constants are determined by three independent measurements made with Z_X (see Fig. 2) replaced with three calibration standards.

Three standards that are readily obtainable and which lead to computational simplicity are an open, short, and termination (R); the reflection coefficients defined with respect to Z are 1, -1, and Γ_R, respectively. A somewhat lengthy computation reveals that

$$\{\Gamma_X\}_R = \frac{(V_X - V_R)(V_\infty - V_0)}{(V_\infty - V_R)(V_X - V_0) + (V_R - V_0)(V_\infty - V_X)}. \tag{29}$$

$\{\Gamma_X\}_R$ is the reflection coefficient of Z_X normalized with respect to R.

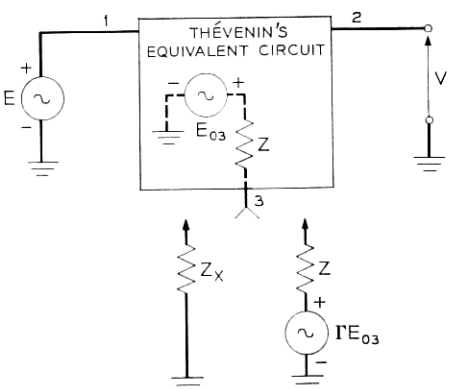

Fig. 17 — Simplified schematic of bridging measurement.

APPENDIX C

Change of the S *Parameter Impedance Normalization*

The voltage S parameters will describe the traveling wave properties of a network terminated in a particular impedance environment. In a different environment the description is no longer valid. Therefore, for example, it is not possible to measure the S parameters of a network in a 50 ohm test set and then use these parameters directly to describe the network performance in a 75 ohm system. It is possible to transform S parameters with one impedance normalization to those of another impedance normalization. These transformations are:

$$\{s_{11}\}_{Z_1,Z_2} = \left\{\frac{\Gamma_1 + s_{11} + \Gamma_1\Gamma_2 s_{22} + \Gamma_2\,\Delta s}{1 + \Gamma_1 s_{11} + \Gamma_2 s_{22} + \Gamma_1\Gamma_2\,\Delta s}\right\}_{Z_{01},Z_{02}} \tag{30}$$

$$\{s_{12}\}_{Z_1,Z_2} = \left\{\frac{s_{12}(1 - \Gamma_1)(1 + \Gamma_2)}{1 + \Gamma_1 s_{11} + \Gamma_2 s_{22} + \Gamma_1\Gamma_2\,\Delta s}\right\}_{Z_{01},Z_{02}} \tag{31}$$

$$\{\Delta s\}_{Z_{01},Z_{02}} = \{s_{11}s_{22} - s_{12}s_{21}\}_{Z_{01},Z_{02}} \tag{32}$$

$$\Gamma_1 = \frac{Z_{01} - Z_1}{Z_{01} + Z_1} \qquad \Gamma_2 = \frac{Z_{02} - Z_2}{Z_{02} - Z_2} \tag{33}$$

where s_{21} and s_{22} are found by transposing subscripts.

These transformations are useful in computing s_{12} of a uniform transmission line normalized with respect to two arbitrary impedances Z_1 and Z_2. The voltage S parameters of a uniform transmission line, normalized with respect to the characteristic impedance of the line, are $s_{11} = s_{22} = 0$ and $s_{12} = s_{21} = e^{-j\theta}$. Then from equation (31),

$$\{s_{12}\}_{Z_1,Z_2} = \frac{e^{-j\theta}(1 - \Gamma_1)(1 + \Gamma_2)}{1 - \Gamma_1\Gamma_2 e^{-j2\theta}}. \tag{34}$$

APPENDIX D

S *Parameters of a Nonideal Transmission Line*

The primary deviation of a physical uniform airline from an ideal airline is caused by the skin effect. The nonideal line is modeled as an ideal line with the added series skin effect resistance of $R_0\omega^{\frac{1}{2}}(1 + j)$ ohms per unit length. The characteristic impedance is

$$Z = Z_0\left[1 + \frac{R_0\omega^{\frac{1}{2}}}{\omega L_0}\right]^{\frac{1}{2}}. \tag{35}$$

The propagation constant is

$$\gamma = -j\omega C_0 Z. \tag{36}$$

The quantities used in the above expressions are defined as:

ω = angular frequency

L_0 = series inductance per unit length of an ideal line

C_0 = shunt capacitance per unit length of an ideal line.

The term $Z_0 = (L_0/C_0)^{\frac{1}{2}}$ = characteristic impedance of an ideal line. The voltage scattering parameters of the nonideal line of length l normalized to two impedances equal to Z are of the simple form

$$s_{11}\,|_{Z,Z} = s_{22}\,|_{Z,Z} = 0 \tag{37}$$

$$\{s_{12}\}_{Z,Z} = \{s_{21}\}_{Z,Z} = e^{\gamma l}. \tag{38}$$

The more useful $s|_{Z_0,Z_0}$ parameters are easily obtained using the transformations of Appendix C. From equation (33) one obtains

$$\Gamma_1 = \Gamma_2 = \frac{Z - Z_0}{Z + Z_0}. \tag{39}$$

For a practical airline $[R_0\omega^{\frac{1}{2}}]/L_0\omega \equiv 2z \ll 1$, allowing for the simplification of expressions (38) and (39) to

$$\Gamma_1 = \Gamma_2 \doteq \frac{z}{2}(1 - j) \tag{40}$$

and

$$\{s_{12}\}_{Z,Z} = \{s_{21}\}_{Z,Z} = e^{-\omega\tau z}e^{-j\omega\tau(1+z)}, \tag{41}$$

$\omega\tau = \omega C_0 Z_0 l$ is the electrical length of the ideal airline. The application of the Appendix C transformations to the $\{s\}_{Z,Z}$ parameters, assuming that the line is electrical short (that is, $z\omega\tau \ll 1$), yields the desired $\{s_{11}\}_{Z_0,Z_0}$ parameters.

For $1/\lambda^2 \gg \omega\tau \gg \lambda^2$

$$\{s_{11}\}_{Z_0,Z_0} = \{s_{22}\}_{Z_0,Z_0} \doteq \lambda(2\omega\tau)^{\frac{1}{2}}\frac{\sin\omega\tau}{\omega\tau}e^{-j\omega\tau+j(\pi/4)} \tag{42}$$

$$\{s_{12}\}_{Z_0,Z_0} = \{s_{21}\}_{Z_0,Z_0} \doteq e^{-\lambda(\omega\tau)^{\frac{1}{2}}}e^{-j\lambda(\omega\tau)^{\frac{1}{2}}}e^{-j\omega\tau} \tag{43}$$

$\lambda = z(\omega\tau)^{\frac{1}{2}}$ is a frequency independent constant of the nonideal line. (See also Ref. 9.)

REFERENCES

1. Geldart, W. J., Haynie, G. D., and Schleich, R. G., "A 50 Hz—250 MHz Computer-Operated Transmission Measuring Set," B.S.T.J., this issue, pp. 1339–1381.
2. Follingstad, Henry G., "Complete Linear Characterization of Transistors from Low Through Very High Frequencies," IRE Transactions on Instrumentation, *I–6,* No. 1 (March 1957), pp. 49–63.
3. Leed, D., and Kummer, O., "A Loss and Phase Set for Measuring Transistor Parameters and Two-Port Networks Between 5 and 250 MC," B.S.T.J., *40,* No. 3 (May 1961), pp. 841–883.
4. Leed, D., "An Insertion Loss, Phase and Delay Measuring Set for Characterizing Transistors and Two-Port Networks Between 0.25 and 4.2 GC," B.S.T.J., *45,* No. 3 (March 1966), pp. 397–440.
5. Kuvokawa, K., "Power Waves and the Scattering Matrix," IEEE Trans. on Microwave Theory and Techniques, *MTT-13,* No. 2 (March 1965), pp. 194–202.
6. Weinberg, Louis, "Fundamentals of Scattering Matrices," Electro-Technology, *80,* No. 1 (July 1967), pp. 55–72.
7. Carlin, H. J. and Giordano, A. B., *Network Theory,* Englewood Cliffs, New Jersey: Prentice-Hall Inc., 1964, pp. 237–255.
8. Evans, J. G., "Linear Two-Port Characterization Independent of Measuring Set Impedance Imperfections," Proc. IEEE, *59,* No. 4 (April 1968), pp. 754–755.
9. Zorzy, J., "Skin-Effect Corrections In Immittance and Scattering Coefficient Standards Employing Precision Air-Dielectric Coaxial Lines," IEEE Trans., on Instrumentation and Measurement, *IM-15,* No. 4 (December 1966), pp. 358–364.